Journal of Tissues and Materials

Characterization and Evaluation of Graphene Oxide Incorporated into Nanofibrous Scaffold for Bone Tissue Engineering

Alireza Safaei Firoozabady[1], Amir Aidun[2,3], Reza Kowsari-Esfahan[4], Azadeh Allahyari[5]

[1]Department of Biomedical Engineering, Science and Research Branch, Islamic Azad University, Tehran, Iran.
[2]National Cell Bank of Iran, Pasteur Institute of Iran, Tehran, Iran
[3]Tissues and Biomaterials Research Group (TBRG), Universal Scientific Education and Research Network (USERN), Tehran, Iran
[4]Department of Cell Engineering, Cell Science Research Center, Royan Institute for Stem Cell Biology and Technology, ACECR, Tehran, Iran
[5]Department of Biomaterials, Faculty of Engineering Science, University of Bayreuth
Correspondence to: Aidun A (E-mail: Aidun_a@aut.ac.ir)

Abstract

Introduction: Many diseases such as cancers, infections and accidents may cause bone defects. So far, many efforts have been made to improve bone tissue engineering, but there are still some ambiguities in this field.

Objective: The aim of the present study is the evaluation of the osteogenic properties of polycaprolactone/Chitosan/Graphene oxide nanofiber scaffold.

Material and Methods: The scaffolds were synthesized by electrospinning method. In this regard, polymers were dissolved in the solvent and then graphene oxide was added into polymeric solution with a ratio of 2% and 4%. The parameters of the scaffold evaluated via scanning field emission electron microscopes (FE-SEM), Fourier transform infrared spectroscopy (FTIR), X-ray Diffraction (XRD), Contact angle, Alizarin red stating, and Alkaline phosphatase (ALP). For evaluation of the cell behavior on the scaffolds, the MG-63 was used.

Result: The findings show graphene oxide not only has a positive effect on the osteogenic properties, but also improve the physico-chemical properties of the scaffolds. The scaffold with 4% graphene oxide make scaffold more hydrophilic in contrast with 2% and 0% scaffold.

Conclusion: The scaffold with 4% graphene oxide shows better morphology, biocompatibility and biological properties in compare to the other scaffolds. In general, the above properties suggest that the GO could enhance osteogenic properties of the scaffolds and GO-incorporated scaffold are a suitable substrate for bone tissue engineering.

Keyword: Bone tissue engineering; Electrospinning; Graphene oxide

Received: 28 December 2018, Accepted: 14 February 2019

DOI: 10.22034/jtm.2019.83189

Tissues & Biomaterials Research Group

1. Introduction

Tissue engineering is a new approach in the field of regenerative medicine, which can be considered as an alternative to current transplants in the near future. Tissue engineering uses polymeric biomaterials known as scaffolds instead of complex living procedures at operation rooms for regeneration of injured tissues or organs. Designed scaffolds must resemble and mimic the structural and functional behavior of host cells. The ECM which is a 3-dimensional complex surrounding cells has a key role in the support and regulation of cells. Depending on certain physical and biochemical features, ECM can result in fabrication of a variety of tissues and organs [1–3] Considering the role of extracellular matrix (ECM) in support and coordinating the regulation of living cell; the polymeric scaffold should be designed accordingly to achieve the best results in tissue engineering. In our body, Depending on certain physical and biochemical features, ECM can result in the fabrication of a variety of tissues and organs [4,5]. Nanofiber scaffolds have been offered as a suitable alternative to replace ECM [6,7]. For tissue engineering, a scaffold should have properties close to the native host tissue, such as biocompatibility and biodegradation [8,9]. A polymer, cannot meet all the requirements of an ECM [10]. Each material has some specific properties which will contribute to the overall efficiency of the scaffold. Due to the synergic effect, the combined effect of materials may surpass the total advantages of materials when considered alone. All polymeric, non-polymeric, synthetic and natural polymers can be used for the fabrication of nanofibrous scaffolds [11–14].

Considering the fact that Polycaprolactone (PCL) has distinctive mechanical qualities and shows acceptable tensile property, it has been widely used in tissue engineering in the last years. PCL is a synthetic linear hydrophobic polymer, and it has the capability to improve bone tissue repair by improving the osteogenic differentiation of human mesenchymal cells [2]. PCL can increase the structural stability of the composite scaffolds. Nevertheless, PCL has a hydrophobic nature and has relatively less potential for cell attachment compared with natural polymers [15]. But the final scaffolds need to better biological properties.

Chitosan is a natural polymer suitable for tissue engineering applications. Chitosan, obtained from chitin, is a biocompatible and biodegradable natural polysaccharide. The similarity between Chitosan and glycosaminoglycan (a major constituent of native ECM) also plays a key role in choosing the material for tissue engineering scaffolds. Suitable cell adhesion and proliferation and remarkable antibacterial effect are caused by Chitosan [16,17]. These polymers in a mixture with PCL can help to final structure of bone scaffold which needed to be addressed.

As synthetic polymer scaffolds have desirable mechanical properties and natural polymers usually are the main source of high biocompatibility and biodegradability, a composite scaffold can be applied to achieve the best result. Furthermore, some features of synthetic and natural polymers such as biological and biomechanical characteristics can be enhanced by functionalization. For the purpose of functionalizing, Graphene oxide (GO) is a notable material that can be used. GO is obtained by the oxidation of graphite. Acquiring a great amount of oxygen causes GO to exhibit great biocompatibility and also bioactivity. It is also considered hydrophilic because of OH groups and COOH groups [18]. In recent years, Graphene and GO have been as a good candidate for biomedical research and especially in the differentiation and stem cells field [19]. GO can enhance certain biomechanical and biological properties when it is used as a reinforcing filler in the structure of polymers. Depending on the interaction between the GO and the polymer matrix, the ultimate nanofibers might show better biological and physico-chemical properties [20,21].

Electrospinning is a simple but versatile technique which can produce nanofibers. And it is also suitable for reaching a combination of the advantages of GO and composite polymers. The electrospun nanofibers exhibit similar features to ECM which mostly consists of nanofibers [15,22].

In previous bone tissue engineering studies composite either two polymers such as collagen/PCL [23,24] and PCL/chitosan [25] were used for fabrication of

scaffold. Some studies also incorporated GO into single or binary polymer nanofibers [26,27]. However, there is no study on the fabrication of GO-incorporated PCL/chitosan electrospun composite scaffold. Hence, this study aimed to fabricate a chitosan/PCL scaffold with different percentage of GO incorporated into the structure.

2. Materials and Methods

2.1. Materials

Polycaprolactone (Mn= 80 kDa), chitosan powder (degree of deacetylation: 90.3±2.1 %), Thiazolyl blue tetrazolium bromide (Mw=414.32 g/mol), Hydrogen peroxide (Mw=34.01 g/mol), Glutaraldehyde and penicillin-streptomycin were all provided by Sigma-Aldrich Co. Ltd. USA. Phosphate buffered saline (powder, pH 7.4) was from Aprin Advanced Technologies Development Co. Ltd. Iran. Dulbecco's Modified Eagle's Medium (DMEM) and Fetal bovine serum (FBS) were purchased from Gibco-BRL Co. Ltd. USA. Ethanol (99.8%, Mw=46.07 g/mol) was purchased from Samchun Pure Chemicals Co. Ltd. South Korea. And finally, MG-63 cells were purchased from the Pasteur Institute of Iran.

2.2. Graphene oxide synthesis

With oxidation of expanded graphite using a modified Hummer [28], GO was prepared. The preparation itself consisted of different steps; first, 1 gram of graphite was added to 1 gram of sodium nitrate in H_2SO_4, then 20 minutes of ice bath condition were performed for stirring the materials. After the dissolution of Granite, 8 g of $KmnO_4$ powder was added to the solution, and the mixture was stirred for 2 hours at 40°C. After the color of the solution turned into brown, H_2O_2 was added to the solution. In order to attain neutrality, the obtained solution was rinsed with 5% HCl and double distilled water.

2.3. Preparation of PCL/Chitosan electrospun scaffold

5 wt% PCL and 2 wt% chitosan were prepared separately by dissolving their powders into a 60% acetic acid / 60% formic acid (1/1, v/v) solvent and 2 hours stirring at 200 rpm at room temperature. The volume ratio of the composite solution was prepared was 2:1 PCL to chitosan. After 12 hours of stirring the components were homogeneously dispersed. After preparing the initial mixture, GO was added in different weight ratios to obtain solutions with various concentrations of 0, 2 and 4 wt%. GO dispersion was mixed into the PCL/chitosan mixture and was for 4 hours stirred. The final solutions named 0%, 2%, 4% were used for electrospinning.

2.4. Electrospinning of the composite scaffold

Final solutions were loaded into 2 ml plastic syringe. Before starting the electrospinning the needle (21G). The flow rate of the solution at 0.5 ml/h was controlled by a syringe pump. 20 kV voltage at the tip of the needle and the 11 cm distance between the collector and the needle were maintained throughout the procedure, and the nanofibers were collected on an aluminum plate at room temperature. Table 1 presents the name of the scaffold according to their components.

2.5. Characterization of prepared scaffolds

2.5.1. Morphology and fiber diameter

The nanostructure of the scaffolds was evaluated by Scanning electron microscope (SEM, Stereoscan S 360-Leica, UK) at a voltage of 15 kV. Gold coated scaffolds achieved by a sputter coater (Emitech

Table 1. The abbreviation and composition of scaffolds

Code	Composition	Graphene Oxide
0% GO	PCL/Chitosan	-
2% GO	PCL/Chitosan /GO	2%
4% GO	PCL/Chitosan /GO	4%

K450X, Ashford, UK) in double 40 second consecutive cycles at 45 mA to produce conductive surface. The nanofibers were studied at 3 random sites. In each site 4 images were taken. The average size of 30 obtained images was analyzed with an image analysis program (KLONK Image Measurement Light, Edition 11.2.0.0).

For identifying how GO embeds on the nanofibers TEM analysis was used. TEM investigation was obtained a transmission electron microscope (CM120, PEG, Philips) at a voltage of 100 kV.

2.5.2. Fourier transform infrared spectroscopy analysis (FT-IR)

Chemical bonds were evaluated performing FTIR spectroscopy over a range between 4000 and 400 cm^{-1}. The preparation of samples performed by mixing 600 mg potassium bromide (KBr) with 2 mg of each raw materials, GO and the scaffolds.

2.5.3. Contact angle

Contact angle test was applied to measure hydrophilicity with a precise goniometer (DSA 100, KRÜSS GmbH Co., Hamburg, Germany). A syringe was placed vertically above the scaffold surface, a 4μL drop of water applied on a 1 cm^2 square sheet of each scaffold. Each measurement was repeated for three times at 3 different sites, and the mean value was reported as the contact angle.

2.5.4. Bioactivity analysis

To probe the effect of the ratio of GO on bioactivity, the sediments of hydroxyapatite (HA) was measured by immersing the scaffolds in 25 ml of SBF solution and incubating them inside a thermoshaker (LS-100, Thermo Scientific, USA) at 25 rpm at 37 °C. The Scaffolds were immersed for 12 hours in SBF10X which was being replaced every 2 hours. FE-SEM then used to detect the formation of appetite on the surfaces, equipped with EDX (FE-SEM, MIRA3, TESCAN Co., Czech Republic). For producing conductive surface and charge reduction, the samples were coated by a gold layer in two 30 seconds cycle at 45 mA[30]. X-ray diffraction (XRD, Philips PW3710) then used to examine the phase analysis of the samples with monochromatic Cu Kα radiation with the performing conditions of 30 mA and 40 kV.

3. Results and Discussion

3.1. Morphology of the electrospun scaffolds

It has been shown that scaffolds comprised of nanofibers are advantageous over microfibrous scaffolds as their nanoscale fibers are in the same order of proteins in native ECM and thus, enhance cell-matrix interactions [33]. As depicted in Figure 1, straight and randomly oriented nanofiber structures were observed in all three groups of 0, 2, and 4% GO-incorporated PCL/Chitosan scaffolds. nanofiber structures, PCL seems to be a fiber diameter controlling parameter, as increasing the PCL ratio would lead to an increase in the fiber diameter. On the other hand, an increment in chitosan ratio may result in beaded structures. Hence, to achieve thin nanofibers while avoiding bead formation in electrospun scaffolds, here we used 1:1 ratio of 10% PCL and 5% Chitosan. SEM micrographs verified that bead morphology was not observed in any of the scaffolds, independent to GO concentration. However, the addition of GO resulted in a slight

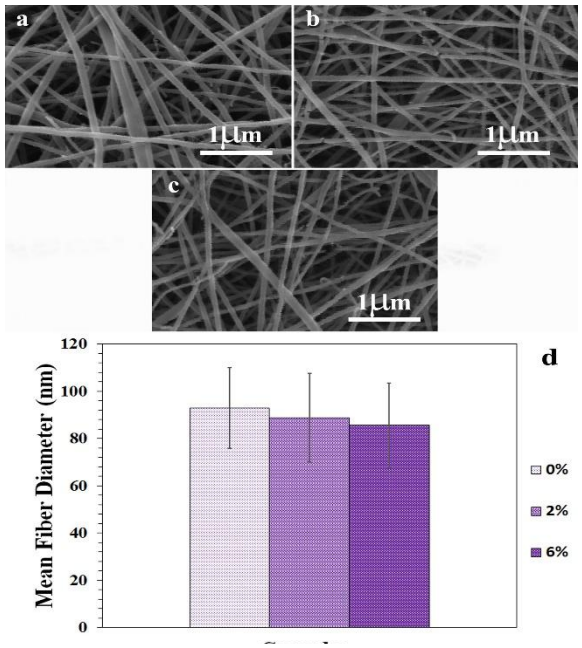

Figure 1. SEM micrographs and nanofiber distribution of electrospun scaffolds 0% GO (a), 2% GO (b), and 4% GO (c) scaffolds. Mean fiber diameter of all scaffolds.

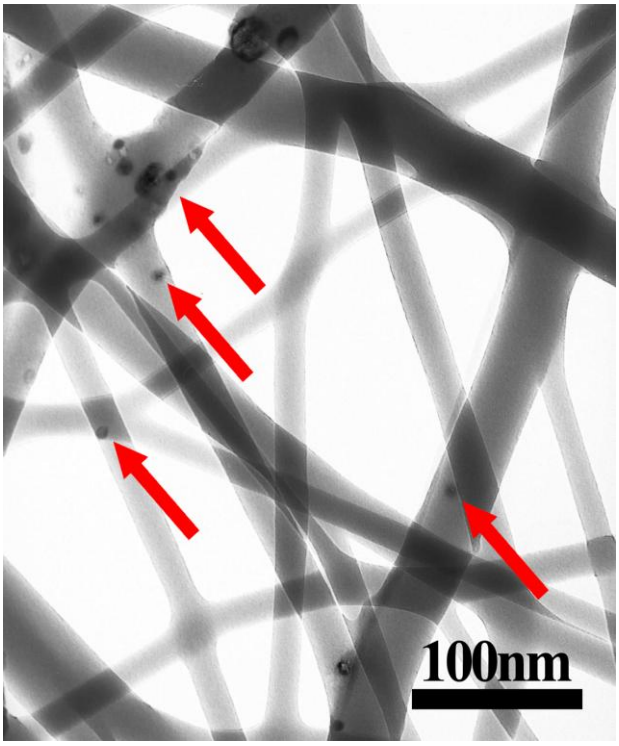

Figure 2. TEM micrograph of the 4% GO scaffold. Darker dot-shaped regions revealed the presence of GO nanosheets.

reduction in the diameter of nanofibers. This could be associated with the fact that GO is a thickening agent and increased viscosity result into thinner electrospun nanofibers. The mean diameter of nanofibers in 0, 2, and 4% GO-incorporated PCL/Chitosan scaffolds are 92.05±17.11, 88.79±18.71, and 85.55±17.90, respectively. (Figure 1d)

For close resemblance of native ECM, a scaffold should also provide an Interconnected, microporous structure to allow cell migration and penetration through the scaffold. This structure could be seen in Figure 1. In the native ECM, lysyl oxidase and collagenase are two regulating factors that locally decrease and increase matrix porosity, respectively [34]. Presence of different porosities is an advantage for a biomimetic scaffold since the native ECM is also non-homogenous in this aspect. The smooth surface of nanofibers in Figure 1b and 1c indicates that GO nanosheets are well embedded in the nanofibers.

Accordingly, a TEM micrograph of the 4% GO-incorporated PCL/Chitosan scaffold (Figure 2), confirms the presence and embedding of the GO nanosheets.

3.2. Characterization of materials

To verify the success of GO synthesis, the FE-SEM, the XRD and the FTIR analysis were conducted. Figure 3a shows GO. As illustrated in Figure 3b, the diffraction peak is located at $2\Theta=15.5°$. XRD pattern clearly demonstrates the formation of GO using the modified Hummers' method. The diffraction peak location and sharpness is also in accordance with previous studies [35–38]. FTIR spectra of GO is shown in Figure 3c. Characteristic peaks of GO appear at approximately 3500 cm^{-1} (hydroxyl groups), at 1630 cm^{-1} (carboxyl groups), and at 1740 cm^{-1} (carbonyl groups). These results, together with XRD analysis confirm the proper synthesis of GO.

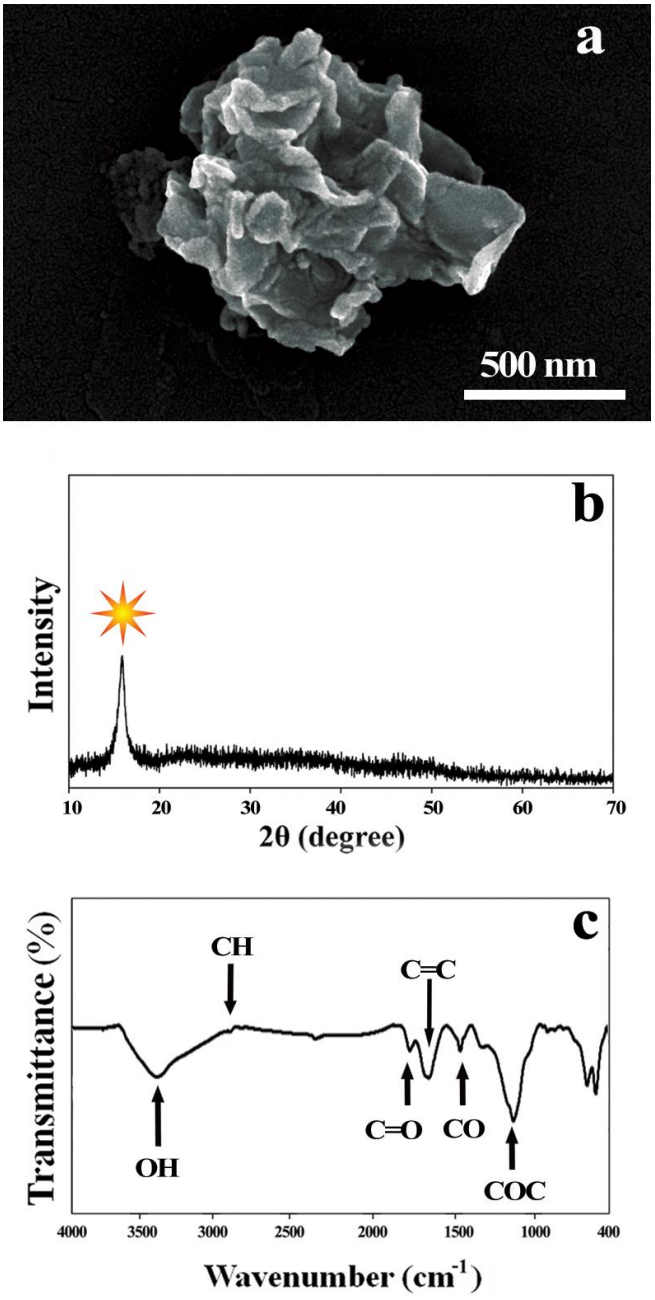

Figure 3. SEM micrograph of the synthesized GO (a), XRD of the GO (b), and FTIR of the synthesized GO.

Figure 4 also illustrates the FTIR spectrum of PCL. Infrared bands at 2922 cm^{-1} (asymmetric stretching), 2864cm^{-1} (symmetric CH_2 stretching), 1722 cm^{-1} (carbonyl stretching), 1288 cm^{-1} (CO and CC stretching) and 1243 cm^{-1} (asymmetric COC stretching) were observed. Characteristic peaks of PCL are in accordance with those described in the literature [39]. Likewise, FTIR spectrum of Chitosan

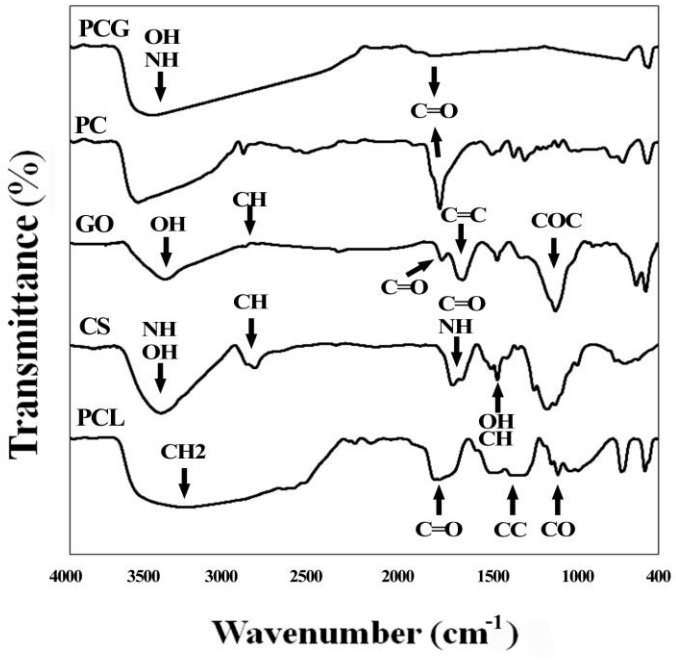

Figure 4. FTIR spectra of polycaprolactone (PCL), chitosan (CS), graphene oxide (GO), PCL/chitosan (PC), and PCL/chitosan/GO4 (PCG) scaffolds in the region 400-4000 cm^{-1}.

was investigated and characterized by its three peaks at 3424 cm^{-1} (hydroxyl groups), 1610 cm^{-1} (primary amine groups), and 1092 cm^{-1} (ether groups) [40].

To study the bonding between PCL and Chitosan, FTIR spectrum of 0% GO sample was analyzed. The infrared band at around 3400 cm^{-1} and 1700 cm^{-1} match with those characteristic peaks of pure PCL and pure Chitosan and shows CH_2 and C=O (carbonyl) in PCL; and OH (hydroxyl groups) and C=O (carbonyl) in Chitosan, respectively.

The FTIR of 0% GO sample shows the carbonyl group shows more intensity at around 1700 cm^{-1}. But, the absence of additional peaks in this sample spectrum demonstrates that the two polymers did not form new covalent bonding. Hence, only physical interactions between functional groups of the polymers would be possible [41].

FTIR spectrum of 4% GO sample scaffold did not add noticeable peaks, compared with 0% GO sample spectrum. However, after GO was added, the sharp peak of C=O in the 0% GO sample and COC in the chitosan disappeared. This indicates a reaction

between carbonyl groups of 0% GO samples and with COC groups of GO.

3.3. Contact angle

In tissue engineering, scaffolds should be preferably hydrophilic as the wettability of the scaffold enhances cell adherence and attachment [42]. However, the PCL component that we used in our hybrid scaffold possesses hydrophobic characteristics due to lack of hydrophilic entities. It has been reported that the water contact angle on a PCL sheet is nearly 120° [43,44]. On the other hand, Chitosan is a hydrophilic biomaterial with contact angles reported from 81.8° [45] to 0° [46]. Hydrophilicity of Chitosan is dependent on many factors, such as the degree of deacetylation [45]. Here we tested the water contact angle on all three scaffolds (Figure 5).

The results of the contact angle are 66.8°, 66.1°, and 58.6° for 0%, 2%, and 4% groups, respectively. Small values of contact angles indicate that all three scaffolds are hydrophilic and thus, suitable for cell adherence. Presence of 4% GO in the scaffold lowered increased the wettability. This improvement could be associated with abundant hydroxyl groups in GO which significantly increased the overall hydrophilicity of the scaffold [47]. Increased wettability in GO-incorporated scaffold was also observed in previous studies [43,47].

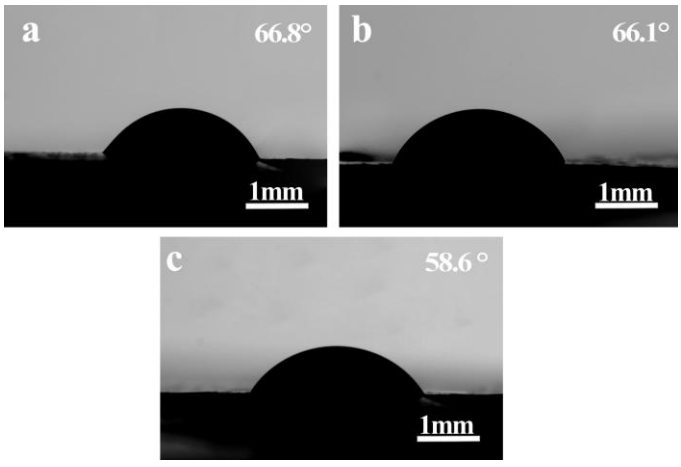

Figure 5. Water drop contact angle images of 0% GO (a), 2% GO (b), and 4% GO (c) scaffolds.

3.4. Bioactivity

In bone tissue engineering, hydroxyapatite sedimentation is a hallmark that shows bioactivity of scaffolds. Here we used FE-SEM to observe and XRD to characterize the phase composition of hydroxyapatite sediments. Figure 6 shows the micrographs taken by FE-SEM. Comparison of the results in panels (b) and (c) with the panel (a) of Figure 6, reveals a clear increase in the amount of sediments in those scaffolds that incorporated GO. To verify the composition of sediments, an XRD analysis was conducted. Previous studies reported that (0 0 2), (2 1 1), (1 1 2), (3 0 0), (2 0 2), (1 3 0), (2 2 2), (2 1 3), and (0 0 4) are the main (h k l) indices in XRD analysis of hydroxyapatite [48]. Here, as shown in Figure 7, two sharp peaks are observable at $2\Theta=32°$ and $2\Theta=45°$, which correspond to (2 1 1) and (2 2 2) planes, respectively.

Biomineralization is an important feature of bone scaffolds as it forms the rigid structure of bones [49]. Providing an in-vitro bone mimetic scaffold improves osteo-activities such as extracellular mineralization. GO improves the mechanical properties of scaffolds to resemble natural bone tissue. Thus, increased mineralization on 2% GO sample and 4% GO sample scaffolds could be linked to the favorable Young's modulus of hybrid scaffold [49].

3.5. Cell adhesion and proliferation

Cell-matrix adhesion, with cooperation with other pathways, regulate the many cell critical processes such as migration, proliferation, differentiation, and homeostasis [34]. This parameter is shown in Figure 8 using FE-SEM imaging. In Figure 8a, adhesion of a cell to 0% GO scaffold could be observed. As reported in the literature, chitosan has shown good adhesion characteristics compared with standard PLL coated culture surfaces [50]. However, an increase in GO concentration further enhances cell adhesion as shown in Figure 8b and 8c, respectively. This could be linked to stepwise improvement in hydrophilicity by the increment in GO concentration [51,52].

Suitability of the scaffolds for proliferation is investigated by MTT assay and its results are shown in Figure 9. For 0% GO scaffold, neither on Day 1 nor

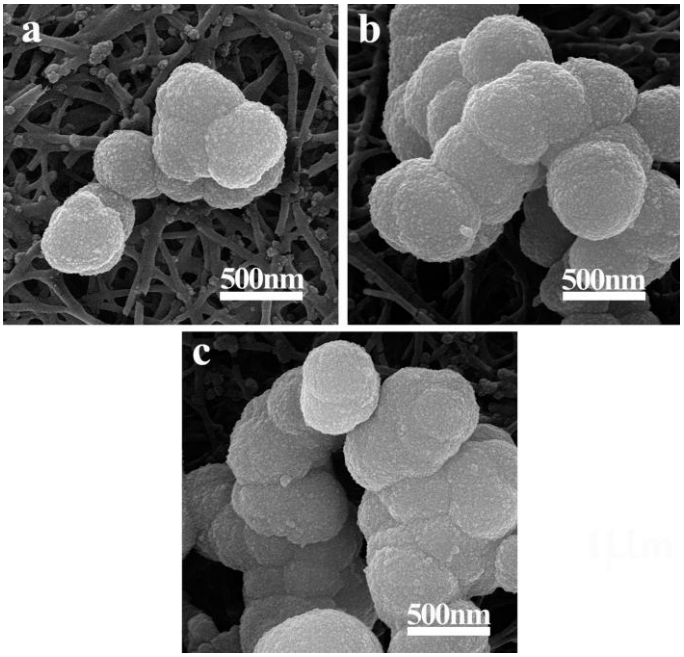

Figure 6. FE-SEM micrographs of mineral sediments on 0% GO (a), 2% GO (b), and 4% GO (c) scaffolds.

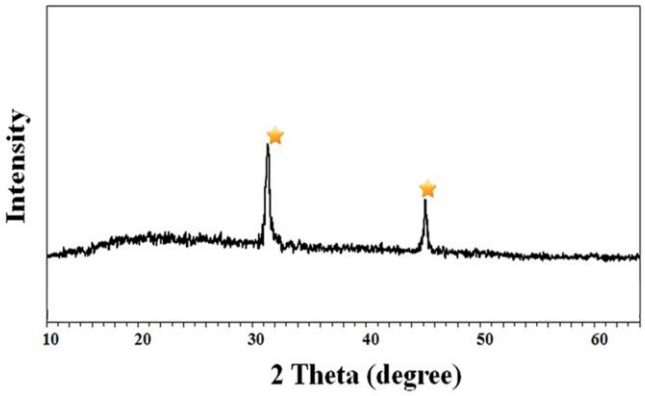

Figure 7. XRD analysis of hydroxyapatite sediments formed on the 4% GO scaffold.

Day 7, measurable improvement in proliferation was not detected compared with control groups ($p>0.05$). However, on Day 1, mean OD for 2% GO increased by 26.56% from 0.423 (control) to 0.576 ($p=0.0018$). Likewise, on Day 1, the mean OD for 4% GO sample also increased to 0.698, showing a 39.39% increase

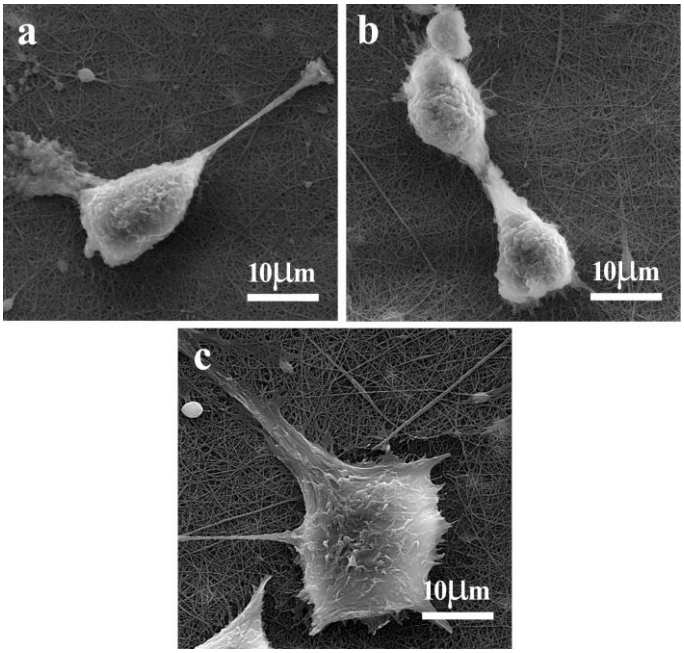

Figure 8. Adhesion of MG-63 cell line on electrospun scaffolds 0% GO (a), 2% GO (b), and 4% GO (c) scaffolds. Cell membrane protrusion indicated cytoskeletal interactions of cells with the scaffold.

compared with the control group ($p<0.0001$). Results of Day 1 also indicated that the addition of GO constantly improved the suitability of the substrate for cell proliferation. On Day 1, 2% GO scaffold showed 20.83% improvement compared with 0% GO scaffold ($p<0.05$), while proliferation on 4% GO scaffold was 17.47 % higher than those on 2% scaffold ($p<0.05$).

We extended the proliferation assay to 7 days, and we observed a similar trend. Once again, 0% sample scaffold showed no significant improvement over the control group. However, proliferation on both 2% and 4% scaffolds increased by 35.92% and 42.65%, respectively compared with the control group ($p<0.0001$). Moreover, the presence of GO augmented the proliferation rate but no measurable difference was observed between 2% and 4% sample scaffolds on Day 7. Results of MTT assay is further endorsed by qualitative Hoechst staining of MG-63 cells on the control plate and 0%, 2%, and 4% samples scaffolds, respectively (Figure 10).

Overall, GO could be identified as a favorable factor for increasing cell proliferation. Interestingly, this

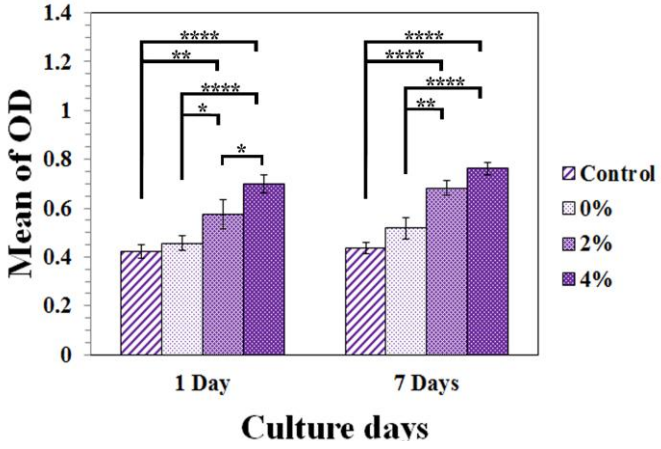

Figure 9. Proliferation of cells on culture dish (control) and GO-incorporated PCL-CS (0%, 2%, and 4% GO).

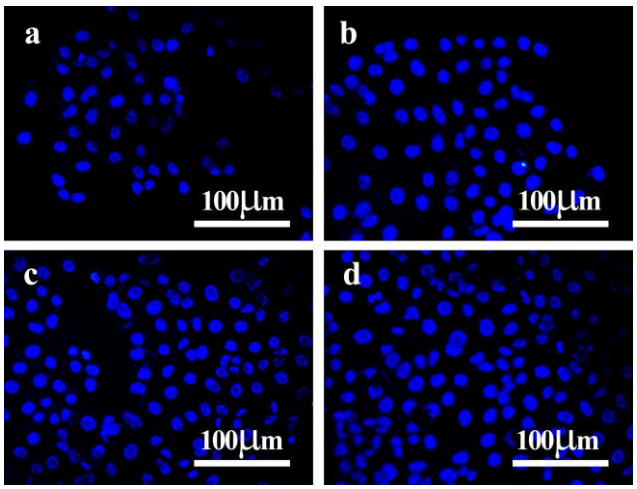

Figure 10. Fluorescence staining of cell nuclei in living cells taken after 24-hours control (a), 0% GO (b) 2% GO (c), and 4% GO (d).

observation is not limited to the cell type. GO-incorporated scaffold improved the proliferation rate for mesenchymal stem cells [53,54], neural [55], skeletal muscle cells [56], and induced pluripotent stem cells (iPSCs) [57]. This phenomenal behavior could be associated with extremely suitable biocompatibility and protein adsorption of GO, and also its hydrophilic nature that improves the overall hydrophilicity of the scaffold [51,52]. Moreover, GO could improve osteogenic differentiation by

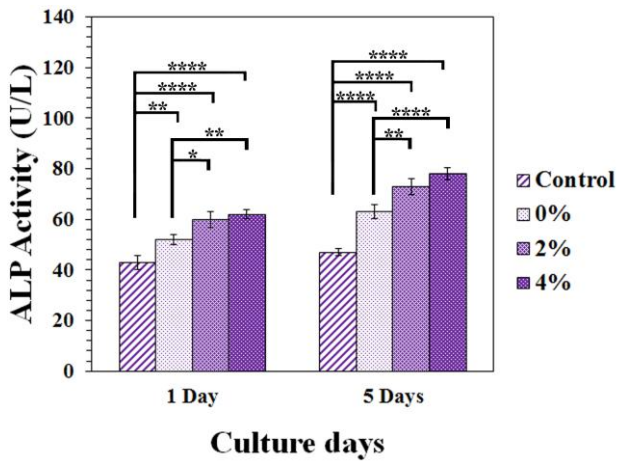

Figure 11. ALP activity of the MG-63 cell line on Day 1 and Day 5 seeded on different substrates.

adsorption of growth factors and local increase of the concentration of those factors such as dexamethasone due to its intrinsic chemical structure [52,58]. These findings suggest GO as an excellent supplement for scaffold for tissue engineering applications.

3.6. Alkaline phosphatase activity and alizarin red assays

To grade the scaffolds based on their osteogenic differentiation capacity for bone tissue engineering purposes, we measured cellular alkaline phosphatase activity as shown in Figure 11. On Day 1 and Day 5, all scaffolds provided better osteogenic environment compared with the control group.

As discussed in the previous section, GO has the capability of protein adsorption, and thus, it gathers biomolecules, providing adhered cells with a local supply of chemical growth factors. Therefore, we expected higher ALP activities in those scaffolds which GO is incorporated. This expectation is confirmed on both Day 1 and Day 5.

According to the findings, the control group has significantly lower ALP activity in both 1st day and 5th day compared with the 0% GO, 2% GO, and 4 % GO group. Figure 11 shows, 0% GO group in the 1st day has significantly (P=0.0183) and (P=0.0026) lower ALP activity compared with the 2% and 4% GO group; also, in the 5th day 0% GO group has significantly

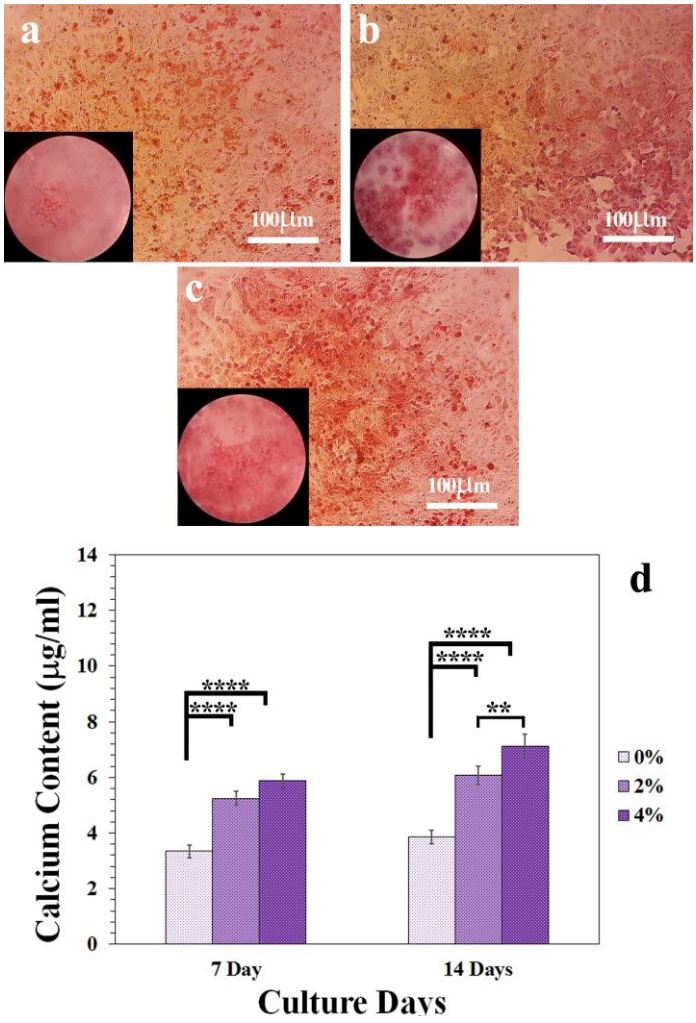

Figure 12. Staining of calcium deposits for 0% GO (a), 2% GO, (b), and 4% GO (c) using Alizarin Red. The quantified result of calcium content on Day 7 and Day 14 are shown in panel (d).

(P=0.0026) and (P<0.0001) lower ALP activity compared with the 2% and 4% GO group. There was no significant difference between 2% GO and 4% GO in both days.

To endorse the results of ALP activity assay, Alizarin Red staining was conducted. In Figure 12, stained calcium deposits are shown qualitatively and quantitatively. Incorporating GO in the scaffolds makes a noticeable difference in the amount of calcium content (Figure 12b and 12c) compared with 0% GO scaffold (Figure 12a). This significant improvement is observable on both Day 7 and 14 (p<0.0001).

It should be noted that in this study, we used the MG-63 cell line, a differentiated osteoblast cell line. Hence, it is expected that the ALP activity was uniform in all cells [59]. As a result, ALP could increase both by an increase in cell number and improvement in the osteogenic capacity of the scaffold. On day 1, the cell number in 4% GO group was significantly higher than 2% GO group (p<0.05). However, the ALP activity of these two groups is similar. The results indicate that GO would improve cell proliferation and ALP activity. According to figure 12, the concentration of GO is not a critical factor in short terms. In contrast, long-term culture of MG-63 cell line proved that 4% GO is superior to 2% GO-incorporated scaffold in terms of calcium deposition (Figure 12d).

4. Conclusion

The present study aims to the evaluation of GO-incorporated into the electrospun scaffold. The findings suggest the GO have a positive effect on the physico-chemical and biological properties. The higher level of the GO by 4% could enhance the osteogenic properties of the scaffold compared with the 2% GO and could be a suitable scaffold.

Conflict of interest

The authors declare that they have no conflict of interests.

Acknowledgments

None declared.

References

[1] Frantz C, Stewart KM, Weaver VM. The extracellular matrix at a glance. J. Cell Sci. [Internet]. 2010;123:4195–4200. Available from: http://jcs.biologists.org/cgi/doi/10.1242/jcs.023820.

[2] Hosseini FS, Soleimanifar F, Aidun A, et al. Poly (3-hydroxybutyrate- co- 3- hydroxyvalerate) improved osteogenic differentiation of the human induced pluripotent stem cells while considered as an artificial extracellular matrix. J. Cell. Physiol. [Internet]. 2018; Available from: https:// onlinelibrary. wiley.com/ doi/abs/ 10.1002/jcp.27807.

[3] Ghorbani F, Zamanian A, Behnamghader A, et al. Bone-like hydroxyapatite mineralization on the bio-inspired PDA nanoparticles using microwave irradiation. Surfaces and Interfaces. 2019;

[4] Jafarkhani M, Salehi Z, Aidun A, et al. Bioprinting in Vascularization Strategies. Iran. Biomed. J. [Internet]. 2019;23:9–20. Available from: http://ibj.pasteur.ac.ir/browse.php?a_id=2599&sid=1&slc_lang=en&ftxt=0.

[5] Metcalfe AD, Ferguson MWJ. Tissue engineering of replacement skin: The crossroads of biomaterials, wound healing, embryonic development, stem cells and regeneration. J. R. Soc. Interface. 2007. p. 413–417.

[6] Nukavarapu SP, Kumbar SG, Brown JL, et al. Polyphosphazene/nano-hydroxyapatite composite microsphere scaffolds for bone tissue engineering. Biomacromolecules. 2008;9:1818–1825.

[7] Morozowich NL, Nichol JL, Allcock HR. Investigation of apatite mineralization on antioxidant polyphosphazenes for bone tissue engineering. Chem. Mater. 2012;24:3500–3509.

[8] Li J, Sun H, Sun D, et al. Biomimetic multicomponent polysaccharide/nano-hydroxyapatite composites for bone tissue engineering. Carbohydr. Polym. 2011;85:885–894.

[9] Tang Y, Zhao K, Hu L, et al. Two-step freeze casting fabrication of hydroxyapatite porous scaffolds with bionic bone graded structure. Ceram. Int. 2013;39:9703–9707.

[10] Ghorbani F, Zamanian A, Aidun A. Bioinspired polydopamine coating-assisted electrospun polyurethane-graphene oxide nanofibers for bone tissue engineering application. J. Appl. Polym. Sci. [Internet]. 2019;1–9. Available from: https://onlinelibrary.wiley.com/doi/abs/10.1002/app.47656.

[11] Aidun A, Zamanian A, Ghorbani F. Novel bioactive porous starch- siloxane matrix for bone regeneration: physicochemical, mechanical, and in- vitro properties. Biotechnol. Appl. Biochem. 2018;

[12] Ghorbani F, Nojehdehyan H, Zamanian A, et al. Synthesis, physico-chemical characteristics and cellular behavior of poly (lactic-co-glycolic acid)/gelatin nanofibrous scaffolds for engineering soft connective tissues. Adv. Mater. Lett. 2016;7:163–169.

[13] McCullen SD, Miller PR, Gittard SD, et al. In situ collagen polymerization of layered cell-seeded electrospun scaffolds for bone tissue engineering applications. Tissue Eng. Part C. Methods [Internet]. 2010;16:1095–1105. Available from: http://www.ncbi.nlm.nih.gov/pubmed/20192901.

[14] Ekaputra AK, Zhou Y, Cool SM, et al. Composite Electrospun Scaffolds for Engineering Tubular Bone Grafts. Tissue Eng. Part A [Internet]. 2009;15:3779–3788. Available from: http://www.liebertonline.com/doi/abs/10.1089/ten.tea.2009.0186.

[15] Song J, Gao H, Zhu G, et al. The preparation and characterization of polycaprolactone/graphene oxide biocomposite nanofiber scaffolds and their application for directing cell behaviors. Carbon N. Y. 2015;95:1039–1050.

[16] Di Martino A, Sittinger M, Risbud M V. Chitosan: A versatile biopolymer for orthopaedic tissue-engineering. Biomaterials. 2005. p. 5983–5990.

[17] Tsai RY, Hung SC, Lai JY, et al. Electrospun chitosan-gelatin-polyvinyl alcohol hybrid nanofibrous mats: Production and characterization. J. Taiwan Inst. Chem. Eng. 2014;45:1975–1981.

[18] Chen Y, Chen L, Bai H, et al. Graphene oxide-chitosan composite hydrogels as broad-spectrum adsorbents for water purification. J. Mater. Chem. A. 2013;1:1992–2001.

[19] Chung C, Kim YK, Shin D, et al. Biomedical applications of graphene and graphene oxide. Acc. Chem. Res. 2013;46:2211–2224.

[20] Jing X, Mi H-Y, Salick MR, et al. Preparation of thermoplastic polyurethane/graphene oxide composite scaffolds by thermally induced phase separation. Polym. Compos. 2014;35:1408–1417.

[21] Dinescu S, Ionita M, Pandele AM, et al. In vitro cytocompatibility evaluation of chitosan/graphene oxide 3D scaffold composites designed for bone tissue engineering. Biomed. Mater. Eng. 2014. p. 2249–2256.

[22] Lim SH, Mao HQ. Electrospun scaffolds for stem cell engineering. Adv. Drug Deliv. Rev. 2009. p. 1084–1096.

[23] Choi DJ, Choi SM, Kang HY, et al. Bioactive fish collagen/polycaprolactone composite nanofibrous scaffolds fabricated by electrospinning for 3D cell culture. J. Biotechnol. 2015;205:47–58.

[24] Zhang Q, Lv S, Lu J, et al. Characterization of polycaprolactone/collagen fibrous scaffolds by electrospinning and their bioactivity. Int. J. Biol. Macromol. 2015;76:94–101.

[25] Ramazani S, Karimi M. Aligned poly(ε-caprolactone)/graphene oxide and reduced graphene oxide nanocomposite nanofibers: Morphological,

mechanical and structural properties. Mater. Sci. Eng. C. 2015;56:325–334.

[26] Jalaja K, Sreehari VS, Kumar PRA, et al. Graphene oxide decorated electrospun gelatin nanofibers: Fabrication, properties and applications. Mater. Sci. Eng. C. 2016;64:11–19.

[27] Cao L, Zhang F, Wang Q, et al. Fabrication of chitosan/graphene oxide polymer nanofiber and its biocompatibility for cartilage tissue engineering. Mater. Sci. Eng. C. 2017;79:697–701.

[28] Zaaba NI, Foo KL, Hashim U, et al. Synthesis of Graphene Oxide using Modified Hummers Method: Solvent Influence. Procedia Eng. 2017. p. 469–477.

[29] Safikhani MM, Zamanian A, Ghorbani F. Synergistic effects of retinoic acid and graphene oxide on the physicochemical and in-vitro properties of electrospun polyurethane scaffolds for bone tissue engineering. E-Polymers. 2017;17:363–371.

[30] Ghorbani F, Nojehdehian H, Zamanian A. Physicochemical and mechanical properties of freeze cast hydroxyapatite-gelatin scaffolds with dexamethasone loaded PLGA microspheres for hard tissue engineering applications. Mater. Sci. Eng. C. 2016;69.

[31] Wang W, Kirsch T. Retinoic acid stimulates annexin-mediated growth plate chondrocyte mineralization. J. Cell Biol. 2002;157:1061–1069.

[32] Stanton L-A, Sabari S, Sampaio A V, et al. p38 MAP kinase signalling is required for hypertrophic chondrocyte differentiation. Biochem. J. 2004;378:53–62.

[33] Li WJ, Laurencin CT, Caterson EJ, et al. Electrospun nanofibrous structure: A novel scaffold for tissue engineering. J. Biomed. Mater. Res. 2002;60:613–621.

[34] Berrier AL, Yamada KM. Cell-matrix adhesion. J. Cell. Physiol. 2007. p. 565–573.

[35] Pandele AM, Ionita M, Crica L, et al. Synthesis, characterization, and in vitro studies of graphene oxide/chitosan-polyvinyl alcohol films. Carbohydr. Polym. 2014;102:813–820.

[36] Yan W, He F, Gai S, et al. A novel 3d structured reduced graphene oxide/TiO2 composite: Synthesis and photocatalytic performance. J. Mater. Chem. A. 2014;2:3605–3612.

[37] Indrawirawan S, Sun H, Duan X, et al. Low temperature combustion synthesis of nitrogen-doped graphene for metal-free catalytic oxidation. J. Mater. Chem. A [Internet]. 2015;3:3432–3440. Available from: http://xlink.rsc.org/?DOI=C4TA05940A.

[38] Liu L, Li C, Bao C, et al. Preparation and characterization of chitosan/graphene oxide composites for the adsorption of Au(III) and Pd(II). Talanta. 2012;93:350–357.

[39] Elzein T, Nasser-Eddine M, Delaite C, et al. FTIR study of polycaprolactone chain organization at interfaces. J. Colloid Interface Sci. 2004;273:381–387.

[40] Wu Y, Yang W, Wang C, et al. Chitosan nanoparticles as a novel delivery system for ammonium glycyrrhizinate. Int. J. Pharm. 2005;295:235–245.

[41] Cooper A, Bhattarai N, Zhang M. Fabrication and cellular compatibility of aligned chitosan-PCL fibers for nerve tissue regeneration. Carbohydr. Polym. 2011;85:149–156.

[42] Kim CH, Khil MS, Kim HY, et al. An improved hydrophilicity via electrospinning for enhanced cell attachment and proliferation. J. Biomed. Mater. Res. - Part B Appl. Biomater. 2006;78:283–290.

[43] Heidari M, Bahrami H, Ranjbar-Mohammadi M. Fabrication, optimization and characterization of electrospun poly(caprolactone)/gelatin/graphene nanofibrous mats. Mater. Sci. Eng. C. 2017;78:218–229.

[44] Ren K, Wang Y, Sun T, et al. Electrospun PCL/gelatin composite nanofiber structures for effective guided bone regeneration membranes. Mater. Sci. Eng. C. 2017;78:324–332.

[45] Hsu SH, Whu SW, Tsai CL, et al. Chitosan as scaffold materials: Effects of molecular weight and degree of deacetylation. J. Polym. Res. 2004;11:141–147.

[46] Gomes S, Rodrigues G, Martins G, et al. Evaluation of nanofibrous scaffolds obtained from blends of chitosan, gelatin and polycaprolactone for skin tissue engineering. Int. J. Biol. Macromol. 2017;102:1174–1185.

[47] Lee EJ, Lee JH, Shin YC, et al. Graphene Oxide-decorated PLGA/Collagen Hybrid Fiber Sheets for Application to Tissue Engineering Scaffolds. Biomater. Res. 2014;18:18–24.

[48] Poinern GJ, Brundavanam R, Le XT, et al. Thermal and ultrasonic influence in the formation of nanometer scale hydroxyapatite bio-ceramic. Int. J. Nanomedicine. 2011;6:2083–2095.

[49] Dong W, Hou L, Li T, et al. A Dual Role of Graphene Oxide Sheet Deposition on Titanate Nanowire Scaffolds for Osteo-implantation: Mechanical

Hardener and Surface Activity Regulator. Sci. Rep. 2015;5.

[50] Gerardo-Nava J, Führmann T, Klinkhammer K, et al. Human neural cell interactions with orientated electrospun nanofibers in vitro. Nanomedicine. 2009;4:11–30.

[51] Qi YY, Tai ZX, Sun DF, et al. Fabrication and characterization of poly(vinyl alcohol)/graphene oxide nanofibrous biocomposite scaffolds. J. Appl. Polym. Sci. 2013;127:1885–1894.

[52] Shin SR, Li YC, Jang HL, et al. Graphene-based materials for tissue engineering. Adv. Drug Deliv. Rev. 2016. p. 255–274.

[53] Nayak TR, Andersen H, Makam VS, et al. Graphene for controlled and accelerated osteogenic differentiation of human mesenchymal stem cells. ACS Nano. 2011;5:4670–4678.

[54] Nair M, Nancy D, Krishnan AG, et al. Graphene oxide nanoflakes incorporated gelatin–hydroxyapatite scaffolds enhance osteogenic differentiation of human mesenchymal stem cells. Nanotechnology. 2015;26:161001.

[55] Park SY, Park J, Sim SH, et al. Enhanced differentiation of human neural stem cells into neurons on graphene. Adv. Mater. 2011;23.

[56] Ahadian S, Ramón-Azcón J, Chang H, et al. Electrically regulated differentiation of skeletal muscle cells on ultrathin graphene-based films. RSC Adv. 2014;4:9534–9541.

[57] Chen G-Y, Pang DW-P, Hwang S-M, et al. A graphene-based platform for induced pluripotent stem cells culture and differentiation. Biomaterials [Internet]. 2012;33:418–427. Available from: http://www.sciencedirect.com/science/article/pii/S0142961211011471.

[58] Akhavan O, Ghaderi E, Shahsavar M. Graphene nanogrids for selective and fast osteogenic differentiation of human mesenchymal stem cells. Carbon N. Y. 2013;59:200–211.

[59] Agarwal T, Kabiraj P, Narayana GH, et al. Alginate Bead Based Hexagonal Close Packed 3D Implant for Bone Tissue Engineering. ACS Appl. Mater. Interfaces. 2016;8:32132–32145.